

Chapter 2

Quartz and MEM Resonators

2.1 The Quartz Resonator

As illustrated by Fig. 2.1(a), a quartz resonator is essentially a capacitor, the dielectric of which is silicon dioxide (SiO_2), the same chemical compound as used in integrated circuits. However, instead of being a glass, it is a monocrystal, a quartz crystal, which exhibits piezoelectric properties. Therefore, a part of the electrical energy stored in the capacitor is converted into mechanical energy.

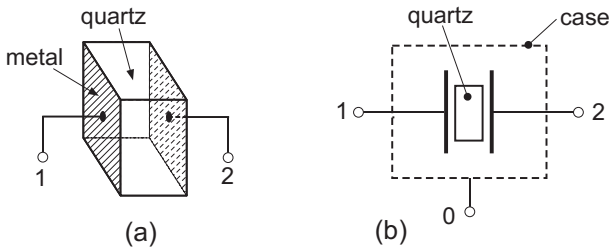


Figure 2.1 Quartz crystal resonator: (a) Schematic structure; (b) symbol.

Whatever the shape of the piece of quartz, it has some mass and some elasticity; it can therefore oscillate mechanically. Unlike simple LC electrical resonators, mechanical resonators always possess several resonance frequencies, corresponding to different possible modes of oscillation (eigenmodes).

Now, if an AC voltage is applied to the capacitor at a frequency close to that of a possible mode, it can possibly excite this mode and drive the quartz resonator into mechanical oscillation.

In addition to its piezoelectric properties, quartz has the advantage of being an excellent mechanical material, with very small internal friction. It has therefore a very high intrinsic quality factor, of the order of 10^6 .

The resonant frequency depends essentially on the shape and the dimensions of the piece of quartz. Possible frequencies range from 1 kHz for large cantilever resonators to hundreds of MHz for very thin thickness-mode resonators.

The exact frequency and its variation with temperature depend on the orientation with respect to the 3 crystal axes. By choosing the optimum mode with an optimum orientation, the linear and quadratic components of the variation of the frequency with temperature can be cancelled, leaving at best a residual dependency of about 10^{-6} from -20 to $+80^\circ\text{C}$.

2.2 Equivalent Circuit

The equivalent circuit of a quartz resonator is shown in Fig. 2.2(a). Although the intrinsic device is a dipole, it is very important in some circuits to model it as a 3-point component, in order to separate the electrical capacitor C_{12} from the parasitic capacitances to the packaging case C_{10} and C_{20} .

If the device is only considered as a dipole, with node 0 floating, then the lumped electrical capacitance is

$$C_0 \triangleq C_{12} + \frac{C_{10}C_{20}}{C_{10} + C_{20}}. \quad (2.1)$$

Each possible mode of oscillation i of the resonator corresponds to a *motional impedance* $Z_{m,i}$ formed by the series resonant circuit $R_{m,i}L_{m,i}C_{m,i}$. The motional inductance L_m is proportional to the mass of the mechanical resonator. The motional capacitance C_m is proportional to the inverse of its stiffness. The motional resistance R_m represents the mechanical losses.

The resonant angular frequency of mode i is given by

$$\omega_{m,i} = 1/\sqrt{L_{m,i}C_{m,i}}, \quad (2.2)$$

and its quality factor by

$$Q_i = \frac{1}{\omega_{m,i}R_{m,i}C_{m,i}} = \frac{\omega_{m,i}L_{m,i}}{R_{m,i}} = \frac{1}{R_{m,i}}\sqrt{\frac{L_{m,i}}{C_{m,i}}}. \quad (2.3)$$

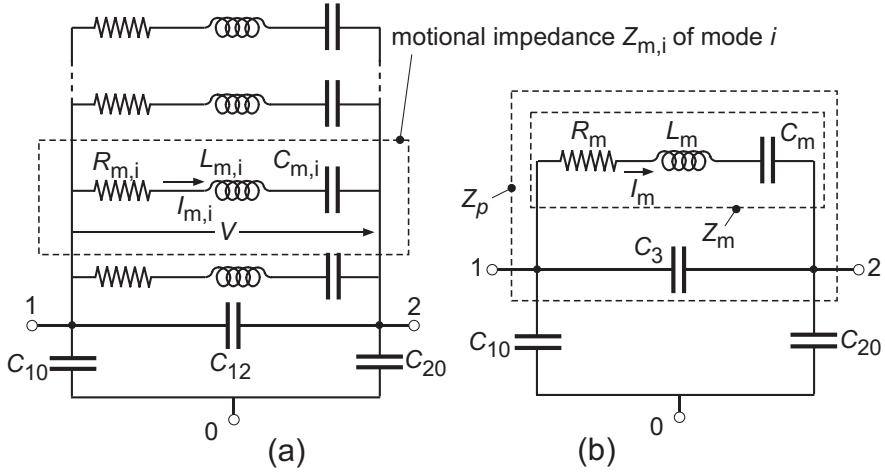


Figure 2.2 Equivalent circuit: (a) of the resonator alone with all possible modes; (b) of a single mode with C_{12} increased to C_3 by external capacitors.

This factor is very large, typically ranging from 10^4 to 10^6 . Whenever needed, this relation between Q , ω_m , R_m and C_m will be used implicitly throughout this book.

The motional current $I_{m,i}$ flowing through the motional impedance $Z_{m,i}$ is proportional to the velocity of mode i . Thus its peak value $|I_{m,i}|$ is proportional to the peak velocity and $|I_{m,i}|/\omega_i$ to the amplitude of oscillation of mode i .

The voltage V across the motional impedances is proportional to the force produced by the piezoelectric effect.

The ratio $C_{m,i}/C_{12} \ll 1$ represents the electromechanical coupling to the mode i . It is always much lower than unity, since it never exceeds the intrinsic coupling coefficient of quartz, which is about 1%. If a mode i is not coupled at all, then $C_{m,i} = 0$ and the corresponding branch disappears from the equivalent circuit.

At this point, two very important remarks must be introduced, since they will greatly simplify the nonlinear analysis of quartz oscillators:

1. Since $Q_i \gg 1$, the bandwidth of Z_m is very narrow. Hence, for frequencies close to the resonance of mode i , the harmonic content of the motional current $I_{m,i}$ is always negligible. Thus, this *current* can be considered *perfectly sinusoidal*, even if the voltage V is strongly distorted:

$$I_{m,i}(t) = |I_{m,i}| \sin(\omega t) \tag{2.4}$$

or, expressed as a complex value

$$I_{m,i} = |I_{m,i}| \exp(j\omega t). \quad (2.5)$$

2. Among the various possible modes of oscillation, we may have the “overtones”, the frequencies of which are close to multiples of that of the fundamental mode. However, because of end effects, these frequencies are not exact multiples of the fundamental. Hence, once a mode is excited, the harmonics that can be produced by the distortion of V cannot excite these overtones. Once oscillation has taken place at one mode, the *other modes* (and thus the other branches in the equivalent circuit) *can be ignored*.

From now on, let us consider only this particular “wanted” mode, and drop the index i in the notations. The equivalent circuit is then reduced to that of Fig. 2.2(b), where C_3 now includes external capacitances possibly added to C_{12} of the resonator itself.

The complex motional impedance is given by

$$Z_m = R_m + j\omega L_m + \frac{1}{j\omega C_m} = R_m + \frac{j}{\omega C_m} \cdot \frac{\omega + \omega_m}{\omega_m} \cdot \frac{\omega - \omega_m}{\omega_m}, \quad (2.6)$$

where the last term has been obtained by introducing (2.2).

Now, because of the very large value of Q , the frequency of oscillation will always be very close to ω_m . It is thus very useful to replace ω by the relative amount of *frequency pulling* (by the circuit)

$$p \triangleq \frac{\omega - \omega_m}{\omega_m} \quad \text{with } |p| \ll 1, \quad (2.7)$$

which, introduced in (2.6), gives almost exactly

$$Z_m = R_m + j \frac{2p}{\omega C_m}, \quad (2.8)$$

where ω can be considered constant with respect to its effect on Z_m . Hence, Z_m is a linear impedance that is *strongly dependent on p* . Indeed, its real part is constant (as long as the quality factor remains constant) but its imaginary part is proportional to p .

2.3 Figure of Merit

An important parameter of quartz resonators (and of all electrostatically driven resonators) is its figure of merit

$$M \triangleq \frac{1}{\omega C_3 R_m} = \frac{QC_m}{C_3}, \quad (2.9)$$

which has a maximum intrinsic value when C_3 is reduced to its minimum value C_{12} , defined as

$$M_0 \triangleq \frac{1}{\omega C_{12} R_m} = \frac{QC_m}{C_{12}}. \quad (2.10)$$

Indeed, M is the maximum possible ratio of currents through Z_m and C_3 . By introducing this definition in (2.8), we can express Z_m normalized to $1/\omega C_3$ as

$$\omega C_3 Z_m = \frac{1}{M} (1 + 2Qpj). \quad (2.11)$$

We can now calculate Z_p , the impedance of the parallel connection of Z_m and C_3 . Assuming ω constant (since $p \ll 1$), it gives, in normalized form:

$$\omega C_3 Z_p = \frac{1 + 2Qpj}{(M - 2Qp) + j} = \frac{M - [4(Qp)^2 - 2MQp + 1]j}{(M - 2Qp)^2 + 1}. \quad (2.12)$$

This impedance becomes real for

$$Qp = \frac{M \pm \sqrt{M^2 - 4}}{4}. \quad (2.13)$$

The negative sign correspond to the *series resonance* frequency, at a value of pulling

$$p_{se} = \frac{C_m}{4C_3} \left[1 - \sqrt{1 - 4/M^2} \right], \quad (2.14)$$

whereas the positive sign corresponds to the *parallel resonance* frequency, at a value of pulling

$$p_{pa} = \frac{C_m}{4C_3} \left[1 + \sqrt{1 - 4/M^2} \right], \quad (2.15)$$

For $M \gg 1$, $p_{se} = 0$; the series resonance frequency is the mechanical frequency of the resonator. But $p_{pa} = C_m/2C_3$; the parallel resonance frequency depends on the electrical capacitance C_3 .

Notice that for $M < 2$, (2.13) has no real solution. The impedance Z_p itself is never real but remains capacitive for all frequencies.

As shown by (2.12), Z_p is a bilinear function of Qp . Now, a property of bilinear functions is to transform circles into circles in the complex plane [8]. Therefore, the locus of $Z_p(Qp)$ for p changing from $-\infty$ to $+\infty$ (circle of infinite radius) is a circle, as illustrated by Fig. 2.3 for the particular case $M = 3$.

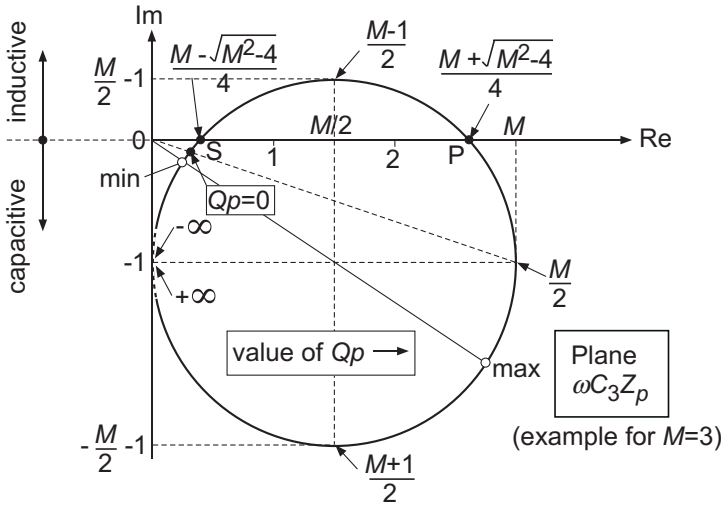


Figure 2.3 Complex plane of $\omega C_3 Z_p(Q_p)$. Notice that this representation is no longer valid for $Q_p \rightarrow \pm\infty$, since it assumes that $|p| \ll 1$.

This circle of radius $M/2$ is centered at $(M/2; -j)$. Since $M > 2$ in this example, the circle crosses the real axis at points S and P corresponding to the series and parallel resonance frequencies given by (2.13). The maximum inductive (normalized) impedance (positive imaginary value) is $M/2 - 1$ and occurs at $Q_p = (M - 1)/2$. The maximum resistive component of the (normalized) impedance is M and occurs at $Q_p = M/2$. Notice that the circular locus is no longer valid for $p \rightarrow \pm\infty$, since ω is no longer constant. The minimum module of the impedance (min) occurs for a slightly negative value of Q_p . The maximum module (max) is larger by M (diameter of the circle).

A small value of M was chosen in Fig. 2.3 in order to make the various points on the circle visible. For larger (and more realistic) values of M , this circle becomes much larger and almost centered on the real axis. The evolution of the module and phase of $Z_p(p)$ for increasing values of M is shown in Fig. 2.4.

As can be seen, for $M \gg 2$ the values of p at series and parallel resonance tend to 0, respectively $M/2Q = C_m/2C_3$, in accordance with (2.13). The corresponding values of Z_p tend to

$$Z_p = \frac{1}{\omega C_3 M} = R_m \quad \text{at series resonance} \quad (2.16)$$

$$Z_p = \frac{M}{\omega C_3} = M^2 R_m \quad \text{at parallel resonance.} \quad (2.17)$$

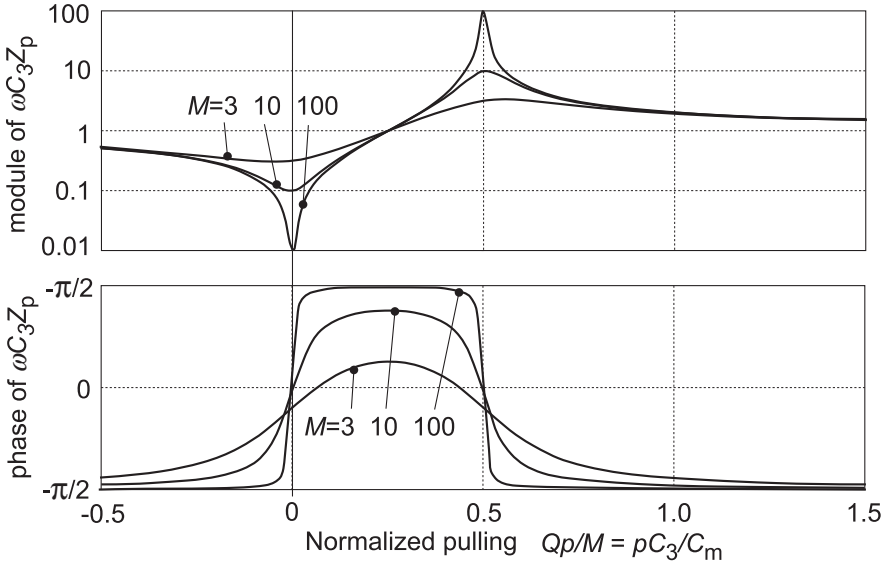


Figure 2.4 Module and phase of Z_p vs. normalized frequency pulling pC_3/C_m .

According to (2.14), (2.15) and (2.9), the exact series and parallel resonance frequencies depend on the electrical capacitance C_3 and the quality factor Q . The calculation of these sensitivities yields:

$$\frac{dp_{se}}{dC_3/C_3} = \frac{C_m}{4C_3} \left[\frac{M}{\sqrt{M^2-4}} - 1 \right] \rightarrow \frac{C_m}{2M^2C_3} \text{ for } M \gg 1, \quad (2.18)$$

$$\frac{dp_{pa}}{dC_3/C_3} = -\frac{C_m}{4C_3} \left[\frac{M}{\sqrt{M^2-4}} + 1 \right] \rightarrow -\frac{C_m}{2C_3} \text{ for } M \gg 1, \quad (2.19)$$

$$\frac{dp_{pa}}{dQ/Q} = -\frac{dp_{se}}{dQ/Q} = \frac{C_m}{C_3} \frac{1}{M\sqrt{M^2-4}} \rightarrow \frac{C_m}{M^2C_3} \text{ for } M \gg 1. \quad (2.20)$$

These sensitivities are plotted in Fig. 2.5 as functions of the figure of merit M . As can be seen, they become rapidly negligible for $M \gg 1$, except that of p_{pa} which tend to $C_m/2C_3$. Indeed, the parallel resonance frequency depends on the series connection of C_m and C_3 .

If M is sufficiently larger than 2, the series resonance frequency becomes independent of the electrical capacitance and of the factor of quality Q . The latter point is important, since some quartz resonators may have a mechanical frequency ω_m very constant with temperature variations, but large variations of their quality factor.

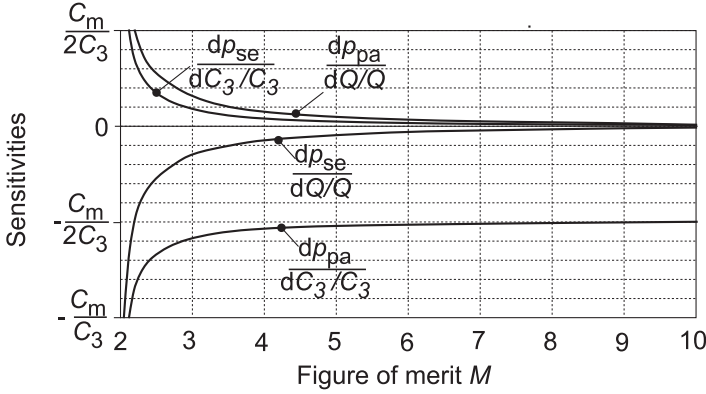


Figure 2.5 Sensitivities of p_{se} and p_{pa} to C_3 and Q .

In order to have a high value of M , the coupling factor C_m/C_3 of the resonator should be sufficiently large according to (2.9). Hence, its intrinsic value itself C_m/C_{12} should already be sufficiently large, since $C_3 > C_{12}$ due to additional parasitic capacitances in the circuit. The figure of merit is further degraded if one of the two “hot” terminals of the resonator is grounded, as in “1-pin” oscillators: indeed, either C_{10} or C_{20} is then connected in parallel with C_3 .

As will be explained later in Chapter 4, the minimization of C_3 is also useful to prevent harmonic currents to flow between nodes 1 and 2, in order to minimize the effect of nonlinearities on the frequency of oscillation.

If the resonator is used as just a dipole, then capacitors C_{10} , C_{20} and C_{12} of Fig. 2.2(a) merge into the single parallel capacitance C_0 defined by (2.1). The corresponding figure of merit is then

$$M_{D0} = \frac{1}{\omega C_0 R_m} = \frac{QC_m}{C_0}. \quad (2.21)$$

In practice, some additional parasitic capacitors will be added to the intrinsic capacitors of the resonators, and the total parallel capacitance C_P is somewhat larger than C_0 , resulting in a figure of merit

$$M_D \triangleq \frac{1}{\omega C_P R_m} = \frac{QC_m}{C_P}. \quad (2.22)$$

2.4 Mechanical Energy and Power Dissipation

Since the quality factor is very large, the energy E_m of mechanic oscillation is almost constant along each period. It is simply exchanged from kinetic energy to potential energy. It is all kinetic energy at the peaks of velocity, and all potential energy at the peaks of amplitude.

Since the motional current I_m represents the mechanical velocity and L_m represent the equivalent mass moving at this velocity, E_m is equal to the peak value of the kinetic energy

$$E_m = \frac{L_m |I_m|^2}{2} = \frac{|I_m|^2}{2\omega^2 C_m} = \frac{QR_m |I_m|^2}{2\omega}, \quad (2.23)$$

where the second form is obtained by introducing (2.2) and the third form by means of (2.3).

Since this energy is proportional to the square of the amplitude, it should be limited to avoid destruction and limit nonlinear effects and aging. But it should be much larger than the noise energy, in order to limit the phase noise, as will be discussed in Section 3.7.

The motional current is sinusoidal, with an RMS value $|I_m|/\sqrt{2}$. The power dissipated in the resonator is thus given by

$$P_m = \frac{R_m |I_m|^2}{2} = \frac{|I_m|^2}{2\omega QC_m}. \quad (2.24)$$

This power must be provided by the sustaining circuit in order to maintain the amplitude of oscillation. Otherwise, at each period of oscillation $2\pi/\omega$, the energy would be reduced by

$$\Delta E_m = \frac{2\pi P_m}{\omega} = \frac{|I_m|^2}{2\omega^2 C_m} \cdot \frac{2\pi}{Q} = \frac{2\pi}{Q} E_m. \quad (2.25)$$

According to (2.23) and (2.24), E_m and P_m can be calculated as soon as $|I_m|$ is known.

2.5 Various Types of Quartz Resonators

Quartz is monocrystal of SiO_2 that has an hexagonal structure with 3 main axes, as illustrated in Fig. 2.6 [9]. The optical axis Z passes through the apex of the crystal. The electrical axis X is a set of three axes perpendicular to Z

that pass through the corners of the crystal. The mechanical axis Y is a set of three axes that are perpendicular to Z and to the faces of the crystal. The electromechanical transducing property comes from the fact that an electrical field applied along one of the X axes produces a mechanical stress in the direction of the perpendicular Y axis.

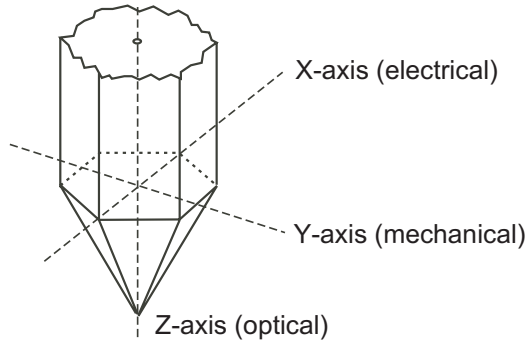


Figure 2.6 Schematic view of a quartz crystal.

Many types of quartz resonators have been developed along the years. They are essentially differentiated by their mode of oscillation, and by the orientation of their cut with respect to the axes. A precise choice of orientation for a given mode is essential to control the variation of the resonant frequency ω_m with that of the temperature.

The variety of possible modes of oscillation is depicted in Fig. 2.7. Each of them corresponds to a practical range of frequency.

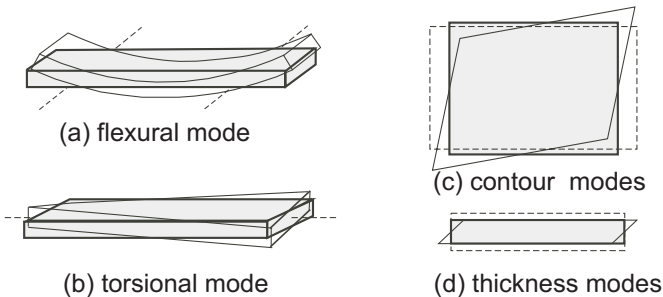


Figure 2.7 Possible modes of oscillation of a quartz resonator.

The flexural mode of Fig. 2.7(a) provides the lowest possible frequencies (down to a few kHz). To minimize losses, it is suspended at its two nodes of

oscillation. The electric field is applied by deposited metallic electrodes. The pattern of these electrodes is optimized to maximize the coupling C_m/C_{12} for the expected fundamental mode. The temperature dependency is a square law of about $-35.10^{-9}/^{\circ}\text{C}^2$ that can be centered at the middle of the temperature range. A vacuum package is needed to obtain a large value of quality factor. This is the type of quartz used for the very first quartz wristwatch in the 60's, with a frequency of 8 kHz [5]. To further reduce its size, the flexural mode resonator can be split into two parallel bars supported by a foot. It becomes a tuning fork resonator [10]. Modern tuning fork resonators are fabricated in a batch process by using the patterning and etching techniques developed for integrated circuits. Their tiny 32 kHz version has become a standard for most electronic watches.

For the same dimensions, the torsional mode depicted in Fig. 2.7(b) resonates at a higher frequency. It can be applied to a tuning fork as well.

Contour modes are obtained by a plate that oscillates within its own plane, as shown by Fig. 2.7(c) (generically, they include the length-mode oscillation of a bar). Resonant frequencies are higher than for the flexural and torsional modes. Best among a large variety of known cuts, the GT-cut [11] eliminates the first, second and third order terms in the variation of ω_m with temperature. The residual variation is of the order of 2 ppm in a 100°C range. But this cut requires a very precise control of the dimensions of the plate, and is therefore very expensive. A less critical solution called the ZT-cut that can be produced in batch was developed more recently [12]. It cancels the first and second order terms, leaving a third order term of only $55.10^{-12}/^{\circ}\text{C}^3$.

High frequencies are obtained by plates resonating in thickness modes as illustrated in Fig. 2.7(d). The most frequent is the AT-cut, that resonates in the thickness shear mode, with a frequency variation of 20 to 100 ppm in a 100°C temperature range. Since the frequency is inversely proportional to the thickness of the plate, very high frequencies are obtained by thinning the vibrating center area of the plate in an "inverted mesa" structure. Fundamental frequencies as high as 250 MHz can then be reached. Harmonic frequencies (overtones) may be used, but their coupling C_m/C_{12} is always smaller than that for the fundamental.

2.6 MEM Resonators

2.6.1 Basic Generic Structure

Very small resonators can be fabricated by using the modern etching techniques that have been developed by the microelectronics industry. For compatibility with integrated circuits, these micro-electro-mechanical (MEM) resonators can be made of polysilicon glass, of aluminum or of silicon itself. The latter exhibits excellent mechanical characteristics, in particular a very high intrinsic quality factor.

However, these materials are not piezoelectric, hence the resonator must be combined with an electromechanical transducer.

The transducer may be a layer of piezoelectric material deposited on the resonator, together with electrodes. The equivalent circuit is then qualitatively the same as that of the quartz resonator illustrated in Fig. 2.2. The coupling factor C_m/C_{12} is reduced by the fact that the transducer only represents a small volume of the resonator, but this may be compensated by using a piezoelectric material with a higher coupling coefficient than that of the quartz. It is thus possible to obtain a sufficiently high value of the intrinsic figure of merit defined by (2.10). The capacitance C_{12} of the transducer should be large enough to limit the reduction of the figure of merit M defined by (2.9) by parasitic capacitors.

Another interesting solution that avoids the need for piezoelectric material is to use an electrostatic transducer. Consider the lumped spring-mass equivalent of such a MEM resonator shown in Fig. 2.8 with its capacitive transducer.

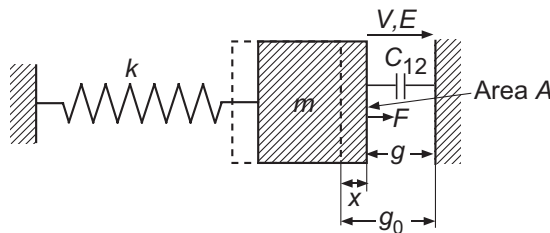


Figure 2.8 Spring-mass equivalent of a MEM resonator with electrostatic transduction.

The equivalent mass of the resonator is m and k is the stiffness of the spring. The angular frequency of mechanical resonance is then given by

$$\omega_m = \sqrt{k/m}, \quad (2.26)$$

whereas the electrical capacitance of the transducer is

$$C_{12} = A\epsilon_0/g, \quad (2.27)$$

where A is the area, g is the gap and ϵ_0 the permittivity of free space.

Statically, the force F due to the electrical field should compensate the force kx of the spring for any value of x , hence:

$$F = QE = C_{12}V^2/g = A\epsilon_0V^2/g^2, \quad (2.28)$$

For a small variation δV of the voltage V around its DC value V_0 , the variation of the force is

$$\delta F = 2A\epsilon_0V_0\delta V/g^2, \quad (2.29)$$

which moves the mass by

$$\delta x = \eta_d \delta F/k, \quad (2.30)$$

where $\eta_d \leq 1$ is a measure of the efficiency of the force to displace the mass, that depends on the mode of oscillation considered ($\eta_d = 1$ in the schematic case of Fig. 2.8). The corresponding variation of the stored mechanical energy E_m is then

$$\delta E_m = \frac{1}{2} \delta F \cdot \delta x = \frac{\eta_d \delta F^2}{2k} = \underbrace{\frac{2\eta_d A^2 \epsilon_0^2 V_0^2}{kg^4}}_{C_m/2} \delta V^2. \quad (2.31)$$

The value of the motional capacitor is then given by

$$C_m = \frac{4\eta_d A^2 \epsilon_0^2 V_0^2}{kg^4}. \quad (2.32)$$

The intrinsic figure of merit of the resonator is then obtained by combining (2.32) and (2.27):

$$M_0 = \frac{QC_m}{C_{12}} = \frac{4\eta_d QA\epsilon_0 V_0^2}{kg^3}, \quad (2.33)$$

or, by replacing the elastic constant by the mass according to (2.26)

$$M_0 = \frac{4\eta_d QA\epsilon_0 V_0^2}{m\omega_m^2 g^3}. \quad (2.34)$$

It can be increased by decreasing the gap or by increasing the bias voltage V_0 . However, the latter is limited by the effect of electrostatic pulling. Indeed,

since V creates a force F that moves the mass by a distance x , the gap g is reduced with respect to its unbiased value g_0 and (2.28) can be rewritten as

$$F = \frac{A\epsilon_0 V^2}{(g_0 - x)^2} = kx/\eta_s, \quad (2.35)$$

where η_s is a measure the efficiency of the force to statically displace the mass ($\eta_s = 1$ in the schematic case of Fig. 2.8). By introducing the normalized position $\xi = x/g_0$, this equation becomes

$$\xi(1 - \xi)^2 = \frac{\eta_s A \epsilon_0}{k g_0^3} V^2 \quad \text{or} \quad V = \sqrt{\frac{k g_0^3}{\eta_s A \epsilon_0}} (1 - \xi) \sqrt{\xi}. \quad (2.36)$$

The system becomes unstable when ξ reaches the limit value ξ_l for which $dV/d\xi = 0$; indeed, for $\xi > \xi_l$, the electrostatic force increases faster than the force of the spring and the mass moves to $x = g_0$. This critical value is reached for

$$\left. \frac{dV}{d\xi} \right|_{\xi=\xi_l} = 0 \quad \text{giving} \quad \xi_l = 1/3. \quad (2.37)$$

Introducing this value in (2.36) gives the limit value V_l of V

$$V_l = \sqrt{\frac{4k g_0^3}{27\eta_s A \epsilon_0}}, \quad (2.38)$$

or, by replacing k by m according to (2.26)

$$V_l = \omega_m \sqrt{\frac{4m g_0^3}{27\eta_s A \epsilon_0}}. \quad (2.39)$$

The bias voltage V_0 can only be some fraction of this limit voltage:

$$V_0 = \alpha V_l \quad \text{with} \quad \alpha < 1. \quad (2.40)$$

By introducing (2.40) and (2.38) in (2.33), we obtain an interesting expression for the all-important figure of merit:

$$M_0 = \frac{QC_m}{C_{12}} = \frac{16}{27} \cdot \frac{\eta_d}{\eta_s} \alpha^2 Q \frac{g_0^3}{g^3} \cong \frac{16}{27} \cdot \frac{\eta_d}{\eta_s} \alpha^2 Q \quad (2.41)$$

where the second expression is a good approximation if $\alpha \ll 1$. Thus, for a given ratio η_d/η_s (which depends on the structure of the resonator), the

intrinsic figure of merit *only depends* on the quality factor and on the fraction α of the limit voltage at which the device is biased. The square of this fraction is the equivalent of the coupling factor of piezoelectric resonators.

According to (2.39), the limit voltage is proportional to the frequency and increases with $g_0^{3/2}$ and $m^{1/2}$. It can be decreased by increasing the area A of the transducer.

For a given frequency, the impedance level (and the value of motional resistor R_m for a given value of Q) is inversely proportional to C_{12} given by (2.27). Hence, it decreases as g/A . Because of the small value of area A possible with a thin resonator and of the difficulty to reduce the gap g much below $1\ \mu\text{m}$, the value of C_{12} is expected to be at least one order of magnitude smaller than for quartz resonators.

2.6.2 Symmetrical Transducers

In many practical cases, the metallic MEM resonator is grounded and is driven by two electrostatic transducers operating in opposite phase according to the spring-mass equivalent depicted in Fig. 2.9. The spring of stiffness k is here represented by a massless flexible blade.

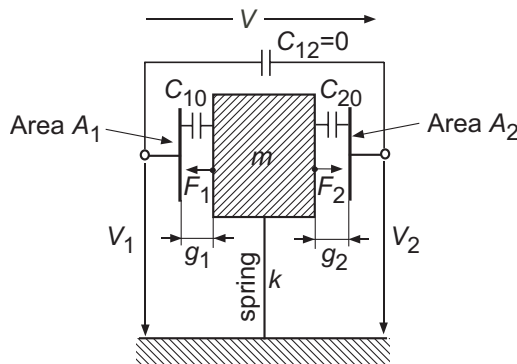


Figure 2.9 Spring-mass equivalent with symmetrical electrostatic transduction.

Using (2.28), the forces produced the two transducers are given by

$$F_1 = A_1 \epsilon_0 V_1^2 / g_1^2 \text{ and } F_2 = A_2 \epsilon_0 V_2^2 / g_2^2. \tag{2.42}$$

The variation of net force $F_1 - F_2$ produced by small variations of V_1 and V_2 around their bias values V_{10} and V_{20} is thus

$$\delta F = \delta F_1 - \delta F_2 = 2\varepsilon_0 \left(\frac{A_1 V_{01}}{g_1^2} \delta V_1 - \frac{A_2 V_{02}}{g_2^2} \delta V_2 \right). \quad (2.43)$$

Let us assume that the bias situation is adjusted for no net force by imposing

$$\frac{A_1 V_{01}}{g_1^2} = \frac{A_2 V_{02}}{g_2^2} = \frac{AV_0}{g^2}. \quad (2.44)$$

Then

$$\delta F = 2A\varepsilon_0 V_0 (\delta V_1 - \delta V_2) / g^2, \quad (2.45)$$

This result is identical to (2.29), since $\delta V_1 - \delta V_2 = \delta V$. Therefore, (2.31) also applies to this symmetrical transducer, for which the motional capacitor is also given by (2.32).

However, there is a major important difference with respect to the non symmetrical case. Indeed, since the body of the resonator is grounded, no capacitive coupling exists between nodes 1 and 2 in Fig. 2.2(a), hence $C_{12} = 0$. The intrinsic figure of merit M_0 is therefore infinite and the overall figure of merit M defined by (2.9) is only limited by all parasitic capacitors contributing to C_3 .



<http://www.springer.com/978-90-481-9394-3>

Low-Power Crystal and MEMS Oscillators
The Experience of Watch Developments
Vittoz, E.

2010, XVIII, 206 p., Hardcover

ISBN: 978-90-481-9394-3